CONTINUUM THEORY FOR STRAIN-SOFTENING

By Zdeněk P. Bažant,[1] F. ASCE, Ted B. Belytschko,[2] M. ASCE, and Ta-Peng Chang,[3] S. M. ASCE

ABSTRACT: In heterogeneous materials such as concretes or rocks, failure occurs by progressive distributed damage during which the material exhibits strain-softening, i.e., a gradual decline of stress at increasing strain. It is shown that strain-softening which is stable within finite-size regions and leads to a nonzero energy dissipation by failure can be achieved by a new type of nonlocal continuum called the imbricate continuum. Its theory is based on the hypothesis that the stress depends on the change of distance between two points lying a finite distance apart. This continuum is a limit of a discrete system of imbricated (regularly overlapping) elements which have a fixed length, l, and a cross-section area that tends to zero as the discretization is refined. The principal difference from the existing nonlocal continuum theory is that the equation of motion involves not only the averaging of strains but also the averaging of stress gradients. This assures that the finite element stiffness matrices are symmetric, while those obtained for the existing nonlocal continuum theory are not. Broad-range stresses are distinguished from local stresses and a different stress-strain relation is used for each—the broad range one with strain-softening, the local one without it. Stability of the material is analyzed, and an explicit time-step algorithm is presented. Finally, convergence and stability are numerically demonstrated by analyzing wave propagation in a one-dimensional bar.

INTRODUCTION

Strain-softening is a decline of uniaxial stress at increasing strain or, generally, a situation where the matrix of tangential elastic moduli ceases to be positive-definite. This phenomenon has been well documented for concrete, rocks and some soils, and it probably also exists in many other materials, including sea ice, filled elastomers, wood, particle boards, paper, some tissues and fabrics, fiber-reinforced composites, fiber-reinforced concretes, asphalt concretes, polymer concretes, various refractory concretes and ceramics, and also some metals. The heterogeneity and brittleness of these materials is the cause of strain-softening. Its mechanism consists of progressive distributed damage, such as dispersed microcracking, void formation or loss of interparticle contacts. Strain-softening occurs not only in tension, but also in compression and shear. Other mechanisms, such as the rate effect, can also be the cause of strain-softening, but these are out of the scope of this work.

Recently it was experimentally established (see, e.g., 1, 3, 5, 6, 17, 20, 56, 63) that strain-softening frequently is distributed over finite-size regions of the material. This suggests that strain-softening should be con-

[1]Prof. of Civ. Engrg., Center for Concrete and Geomaterials, Northwestern Univ., Evanston, Ill. 60201.

[2]Prof. of Civ. Engrg., Center for Concrete and Geomaterials, Northwestern Univ., Evanston, Ill. 60201.

[3]Grad. Research Asst., Northwestern Univ., Evanston, Ill. 60201.

Note.—Discussion open until May 1, 1985. Separate discussions should be submitted for the individual papers in this symposium. To extend the closing date one month, a written request must be filed with the ASCE Manager of Technical and Professional Publications. The manuscript for this paper was submitted for review and possible publication on January 16, 1984. This paper is part of the *Journal of Engineering Mechanics*, Vol. 110, No. 12, December, 1984. ©ASCE, ISSN 0733-9399/84/0012-1666/$01.00. Paper No. 19333.

sidered as a continuum property. Serious theoretical and computational difficulties arise, however, when either the local continuum theory or the existing nonlocal continuum theory is used. The purpose of this study is to construct a theory that circumvents these difficulties. This theory, briefly outlined in Ref. 6, involves a new type of nonlocal continuum.

Present Status of Strain-Softening Theory

Ever since Hadamard (33) pointed out that the wave velocity becomes imaginary and the differential equation of motion changes from hyperbolic to elliptic if the tangent moduli matrix ceases to be positive-definite, strain-softening has been widely regarded as inadmissible in continuum mechanics (36,50,61,62). In the context of plasticity, strain-softening has been ruled out since it invalidates the uniqueness theorem, bounding principles and normality rule (2,53). The difficulties caused by strain-softening have been intensely debated at recent conferences, particularly with regard to large-scale finite element computation. Sandler and Wright (59), Hegemier (35), Wu and Freund (64) and others (9) demonstrated, by examples, various unpleasant features, such as the discontinuous dependence of the response on initial or boundary conditions, and the associated instabilities. Sandler (59) pointed out that dynamic problems with continuum strain-softening are not mathematically well posed.

The relevance of Hadamard's point is questionable, however, since it ignores the fact that the unloading modulus is positive even in the strain-softening range [see Fig. 1(*a*) rather than Fig. 1(*b*)]. By static analysis, in which this fact was taken into account, it was shown (1,3,20) that, for the classical local continuum, a state of uniform strain whose value is in the strain-softening range is unstable, and that the instability mode represents strain localization into a layer of the smallest possible thickness (1,3,20). For this type of strain localization (1), nonuniqueness of the tangent modulus due to its different values with opposite signs for

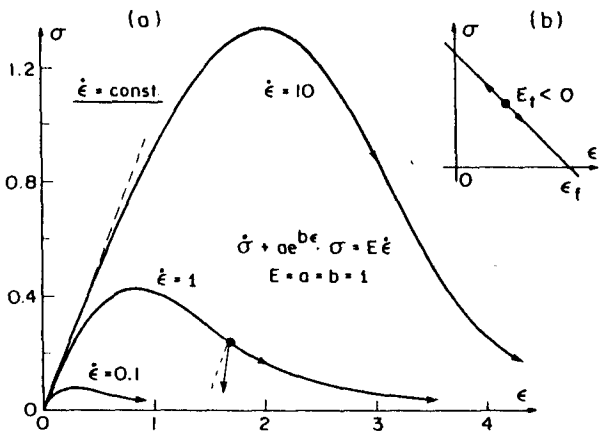

FIG. 1.—Inadequate Models for Strain-Softening: (*a*) Rate Effect; (*b*) Linear Material of Negative Modulus

loading and unloading is essential. However, geometrical nonlinearity due to finite strain is not essential because the magnitudes of the moduli are much larger than those of stresses. This contrasts with another kind of strain-localization instability studied by Rice and Rudnicki (54,57,58), which is caused by finite-strain geometrical nonlinearity at a very small but still positive tangent modulus. Static strain-softening was also studied for bending problems in which it was either assumed to localize (28,29,48,49) or proven to localize (1).

Dynamic strain-softening in local continuum has been analyzed in Ref. 9, in which an exact solution has been obtained for a one-dimensional bar in which two step waves of strain propagate toward each other. For certain magnitudes of the strain step the incoming waves are elastic, but as they meet, strain-softening is produced. The stress is then instantly reduced to zero, and strain-softening remains subsequently localized within a single cross-section plane, from which unloading step waves of strain are emitted. Contrary to some recent opinions, the problem formulation does not appear to be mathematically meaningless since a unique solution is obtained for given initial and boundary conditions, and since the usual explicit step-by-step algorithm yields results which converge to the exact solution. The exact solution does not depend continuously on the boundary condition, which means that, in mathematics terminology, the problem is not well-posed. From the physical viewpoint, however, this is not disturbing, although another aspect is—the fact that the energy consumed by failure due to strain-softening is zero, according to the exact solution (9). This fact, a result of the impossibility of obtaining a finite-size strain-softening region, is an unrealistic feature of local continuum, not representative of real materials.

To achieve finite energy consumption, the artifice of imposing a certain minimum size, l, of the strain-softening region (crack band) was proposed in the blunt crack band model (1) and later extensively developed (3,5,6,10,11,12,15,17,19,21,26,51,55) for the purpose of finite element modeling. Good agreement with essentially all experimental results for concrete or rock fracture has been achieved (17,19), including the maximum load data and the R-curve data for various fracture specimens, as well as the crack shear data (15) and the deflection data for partially cracked structures (18). A general dimensional analysis based on the hypothesis of constant finite width of the front of the strain-localization (cracking) band has resulted in a simple formula for the size effect (4), which was found to agree well with various existing failure data, such as diagonal shear failure data for beams (16).

The use of strain-softening in finite element codes was shown to be unobjective with regard to the analyst's choice of the mesh size (10,11,12,17,27,56), and to converge with decreasing mesh size to a physically incorrect solution (vanishingly small failure load). The artifice of enforcing a certain constant minimum width of the strain-softening band removes these incorrect features but makes it impossible to obtain with the local continuum theory a detailed resolution of the stress and strain fields within and near the strain-softening region.

Some workers, emphasizing that strain-softening does not exist on the microstructural level, have recently suggested that strain-softening be treated as point defects, such as progressively developing microcracks,

which represent the true physical source of macroscopic strain-softening. However, structural analysts need a smeared-out overall description, such as that provided by a macroscopically equivalent continuum. There is no hope of directly treating in structural analysis these numerous point defects, with the attendant inhomogeneities of the microstructure, individually.

Others (59) have suggested that strain-softening be treated as a consequence of a rate effect, i.e., by means of viscoplasticity. Yet it seems that a sufficiently realistic model cannot be achieved in this manner. For instance, consider that $E\dot{\epsilon} = \sigma + f(\epsilon)\sigma/\tau_1$, which is visualized by the Maxwell model with a nonlinear dashpot and a linear spring, in which σ = uniaxial stress; ϵ = strain; E and τ_1 = material constants; superior dots denote time derivatives; and $f(\epsilon) = a \exp(b\epsilon)$ in which a, b = constants. Integration of this differential equation for a constant strain rate $\dot{\epsilon}$ (i.e., $\epsilon = \dot{\epsilon}t$, t = time) yields the curves in Fig. 1(*a*) which look like strain-softening diagrams; these curves correspond to three different strain rates: $\dot{\epsilon} = 0.1$, 1, and 10 (and $E = a = b = 1$). What strikes the eye is the enormous rate effect. Could these curves represent the same concrete or rock for tests which take, e.g., 0.1 min, 1 min and 10 min to failure? Certainly not. There is, of course, a strain-rate effect in concrete or rock, but an order of magnitude weaker. [Aside from that, the unloading modulus predicted in the strain-softening range is much too high; see Fig. 1(*a*).] Using another model, e.g., the Kelvin model (59) or the Maxwell chain model, one can obtain stress-strain diagrams with a realistic rate effect, but then it appears impossible to get strain-softening without assuming the spring moduli to become negative.

In recent debates it has often been emphasized that the true stress, which acts within small material elements lying between the defects, never decreases, and that strain-softening is merely due to a decrease of the net resisting area fraction within the material. This is, of course, correct; however, the mathematical formulation with a net resisting area fraction that is variable and approaches zero is tantamount to formulating a strain-softening constitutive law. Consequently, this approach, taken in continuous damage mechanics (38,39,42,44,45,46,52), inherits all of the difficulties of strain-softening, except when apparent strain-softening is actually stress relaxation due to creep (44,45).

Much inspiration for the present theory came from Burt and Dougill (25). Their model seems to be the only one where a finite-size strain-softening region was obtained rather than enforced (e.g., enforced by meshing or by lack of stability checks). They analyzed, by computer, a random two-dimensional network whose joints are placed at random locations over a rectangular domain. They considered all pairs of joints with a distance less than a certain constant, l, made a random selection among all such pairs, and introduced between each pair connecting pin-jointed elastic struts whose stiffnesses and strength limits were generated randomly according to prescribed normal distributions. After reaching the strength limit, the force in the strut was assumed to drop immediately to zero. For the present work, it is interesting that the struts overlapped at numerous points without being joined. Although this model could not have exhibited the correct elastic Poisson ratio (which must have been 1/3), the response was remarkably similar to concrete, including strain-softening and the effects of the degree of heterogeneity and the size of specimen.

Classical Nonlocal Continuum Theory

From Burt and Dougill's work it is clear that a statistical heterogeneity of the material must be somehow reflected in the continuum model. Statistically heterogeneous materials may be characterized (though not completely) by the properties of the so-called representative volume (34), which is defined as the volume V (e.g., a sphere) of the smallest size l for which the statistical characteristics of the microstructure are essentially the same regardless of the location of the center of this volume. The macroscopic strain, ϵ, and stress, σ, may be regarded as certain averages of the microscopic (actual) strains and stresses taken over volume V. If the strain field is macroscopically homogeneous (uniform) or nearly homogeneous, the constitutive relation may be formulated as a relation between $\epsilon(x)$ and $\sigma(x)$ at the same location x. However, if high gradients of ϵ exist, statistical analysis shows (23,40) that this is no longer adequate, and that the entire macroscopic (smoothed) stress distribution over V should be related to the entire macroscopic (smoothed) strain distribution over V.

The simplest theory of this type, and the only one used so far to solve field problems (31), is the theory of nonlocal continuum introduced by Kröner, Kunin, Krunhansl and others (23,40,41,42,43,47) and developed in detail by Eringen et al. (30,31,32). In this theory the stress-strain relation is written as $\boldsymbol{\sigma}(\mathbf{x}) = \int_B \mathbf{D}(\mathbf{x}, \mathbf{x}')\boldsymbol{\epsilon}(\mathbf{x}')dV$ in which $\mathbf{x}$ is the coordinate vector; $\boldsymbol{\sigma}$, $\boldsymbol{\epsilon}$ are the column matrices of macroscopic stress and strain components; $\mathbf{D}$ is the square matrix of elastic moduli; and B is the whole domain of the body. In all applications so far it has been assumed that $\mathbf{D}(\mathbf{x}, \mathbf{x}') = \mathbf{C}(\mathbf{x})\alpha(s)$ in which $s = |\mathbf{x}' - \mathbf{x}|$; $\alpha(s)$ is a given weighting function; and $\mathbf{C}$ is a matrix of elastic moduli independent of s. The one-dimensional small-strain formulation then is

$$\sigma(x) = E\,\bar{\epsilon}(x), \quad \bar{\epsilon}(x) = \int_{-\infty}^{\infty} \epsilon(x + s)\alpha(s)ds = \bar{H}\,\epsilon(x) \qquad (1)$$

in which $\sigma(x)$ = stress (macroscopic, smoothed); E = elastic modulus, interpreted as the secant modulus if the stress-strain relation is nonlinear; $\epsilon(x)$ = strain (macroscopic, smoothed); $\bar{\epsilon}(x)$ = weighted average of strain; $\bar{H}$ = averaging operator; and $\alpha(s)$ = given weighting function, which is zero or negligibly small outside the region $-l/2 \le x \le l/2$ constituting the representative volume, and is such that $\int_{-\infty}^{\infty}\alpha(s)ds = 1$ and $\alpha(s) = \alpha(-s)$. The equation of motion and the strain definition are considered as usual:

$$\frac{\partial\sigma(x)}{\partial x} = \rho\frac{\partial^2 u(x)}{\partial t^2}, \quad \epsilon(x) = \frac{\partial u(x)}{\partial x} \qquad (2)$$

in which u = displacement (macroscopic, smoothed); ϵ = local strain (smoothed); t = time; and ρ = mass density.

Extensive dynamic one-dimensional finite element calculations were carried out for this classical nonlocal continuum theory, in which E was

introduced as a function of $\bar{\epsilon}$. It appeared, however, that this theory cannot model strain-softening. Just like for the ordinary local continuum, a strain-softening region of finite width cannot be obtained and the occurrence of strain-softening leads immediately to a localization of strain into a single finite element no matter how small the element is. Thus, the width of the strain-localization region and the energy consumed by strain-softening failure converge to zero as the element size is decreased to zero, and the response exhibits extreme noise which is probably due to instability. Thus, another version of nonlocal continuum theory is needed.

Basic Hypothesis and Mean Strain

The strain averaging in Eq. 1 is usually interpreted to mean that strain $\epsilon(x)$ at point x depends on the strains $\epsilon(x + s)$ at other points of $x + s$. This interpretation is unrealistic, however, because the material at one point cannot "feel" the strain at another point. Strain averaging should be physically interpreted through its relation to the change of distance between points $x + s$ and $x - s$. This may be brought to light by substituting $\epsilon(x + s) = \partial u(x + s)/\partial s$ in Eq. 1 and integrating by parts. Assuming that the weights $\alpha(s)$ are zero outside the interval $-l/2 \leq s \leq l/2$, in which l is a certain characteristic distance, and noting that the symmetry property, $\alpha(s) = \alpha(-s)$, requires antisymmetry of the derivative, $d\alpha(s)/ds = -d\alpha(-s)/ds$, we thus obtain

$$\bar{\epsilon}(x) = \frac{1}{l}\left[u\left(x + \frac{l}{2}\right) - u\left(x - \frac{l}{2}\right)\right] w\left(\frac{l}{2}\right) + \int_0^{l/2} \frac{1}{2s}\,[u(x + s) - u(x - s)]w(s)ds \quad \ldots\ldots (3)$$

in which $w(s)$ are weights such that $w(l/2) = l\alpha(l/2)$ and, for $0 \leq s < l/2$, $w(s) = -2s\, d\alpha(s)/ds \geq 0$.

For the sake of simplicity, we will assume that the weights, $\alpha(s)$, are uniform, i.e., $\alpha(s) = 1/l$. Eq. 3 then becomes

$$\bar{\epsilon}(x) = \frac{1}{l}\int_{-l/2}^{l/2} \epsilon(x + s)ds = \frac{1}{l}\left[u\left(x + \frac{l}{2}\right) - u\left(x - \frac{l}{2}\right)\right] \quad \ldots\ldots (4)$$

which will be called the mean strain. Eq. 4 indicates that the overall stress σ depends on the relative displacement between the ends of segment l or, more precisely, that the stress resultant σA (a force) over the cross section area A of the representative volume depends on the change of length of segment $\overline{12}$ in Fig. 2(*a*). The important point (which will lead us later to the concept of imbricated elements) is that points 1 and 2 must be *symmetrically* located with regard to cross section $\overline{PQ}$; a change of length $\overline{34}$ in Fig. 2(*a*) determines *not* the stress on the cross section $\overline{PQ}$, but the stress on cross section $\overline{RS}$.

To crystallize the preceding thought, we may pronounce, for a one-dimensional continuum, the following hypothesis, in which l is a material property (a constant) called the characteristic length.

Hypothesis I.—The stress $\sigma(x)$ at any point x (except in a boundary

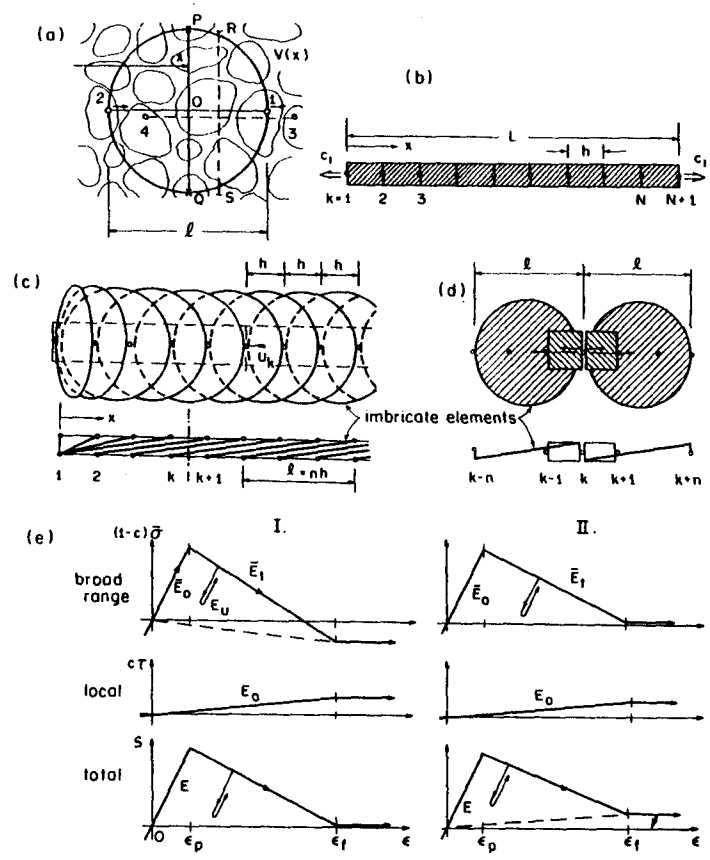

FIG. 2.—Imbricate Nonlocal Continuum: (*a*) Representative Volume; (*b–d*) System of Local and Imbricate Elements; (*e*) Stress-Strain Diagrams

layer of thickness $l/2$): (1) Depends on the change of distance between points $x + l/2$ and $x - l/2$; but (2) does not depend on the change of distance between any other two points lying a finite distance apart.

It follows that the continuum must consist of all possible (continuously distributed) material elements connecting any two points lying at distance l from each other. Moreover, part 2 of Hypothesis I suggests that these elements should have a parallel and overlapping (imbricated) arrangement, in which the neighboring elements are not mutually joined [Fig. 2(*c*)]. A proof that such an imbricated arrangement unequivocally follows from Hypothesis I may be given by variational calculus (as is shown in a subsequent paper in this issue).

Before proceeding further, we should comment on the choice of the weighting function, $\alpha(s)$. Uniform weights are the simplest, but they may lead to instability (13). The equation $\int_l \epsilon(x + s)\alpha(s)ds = 0$ for $\alpha(s) =$ constant has a nonzero solution of the type $\epsilon(x) = A \sin(2\pi x/l)$ (with any A), which means that nonzero $\epsilon(x)$ can happen at zero stress and zero energy, for which $\bar{\epsilon}(x) = 0$. To avoid this instability, other weighting

functions, such as the normal (Gaussian) distribution (13), may be used. However, to keep the finite element formulation simple, uniform weights $\alpha(s)$ (Eq. 4) are preferable. The aforementioned stability problem may then be overcome by simultaneous use of the local strain, $\partial u/\partial x$.

The magnitude of l may be experimentally calibrated according to fracture tests of similar specimens of different sizes. Approximately, l for concrete is three times the maximum aggregate size.

Discrete Model

Although our ultimate objective is a continuum model, it is instructive and easier to derive it as a limit of a discrete model. We restrict attention to a one-dimensional continuum and consider a bar of a unit cross section. We subdivide the length coordinate x by nodes $k = 1, 2, 3, \ldots$ into equal segments of length h [Fig. 2(*b*) and (*c*)], subjected to the condition that $l = nh$ in which n is an integer and l is the given size of the representative volume. The mean strain $\bar{\epsilon}$, as given by the difference expression (Eq. 4), is the strain obtained in one-dimensional elements of length l. These elements are shown as circles in Fig. 2(*c*). They span over n segments h, and are connected only at their ends, so that the strain in each of them is uniform. These elements overlap, i.e., are *imbricated* (as shown in Fig. 2(*c*), where the nodes above each other have the same displacement). A cross section between two nodes [Fig. 2(*c*)] is intersected by a total of n identical imbricate (regularly overlapping) elements acting in parallel. The combined cross-section area of all imbricate elements intersected by the same cross section of bar must be a constant, independent of n. Denoting this combined area as $(1 - c)$ in which $0 \leq c \leq 1$, we see that the cross section of each imbricate element must equal $(1 - c)/n$. Obviously it decreases as the subdivision of l is refined and tends to 0 as $n \to \infty$.

Although n imbricate elements are intersected by each cross section between the nodes [Fig. 2(*c*) and (*d*)], only two of the elements are connected to each node, one from each side [Fig. 2(*d*)]. The stresses in these two elements, which will be called the broad-range stresses, are

$$\sigma_k = \bar{E}(\epsilon_k)\bar{\epsilon}_k, \quad \sigma_{k-n} = \bar{E}(\epsilon_{k-n})\bar{\epsilon}_{k-n} \qquad (5)$$

$$\text{in which} \quad \bar{\epsilon}_k = \frac{1}{l}(u_{k+n} - u_k), \quad \bar{\epsilon}_{k-n} = \frac{1}{l}(u_k - u_{k-n}) \qquad (6)$$

in which $\bar{E}$ = the elastic modulus, interpreted as the secant modulus if the material behaves nonlinearly. The nodal forces at node k arising from these two elements [Fig. 3(*d*)] are

$$F_k^+ = \frac{1-c}{n}\sigma_k, \quad F_k^- = \frac{1-c}{n}\sigma_{k-n} \qquad (7)$$

We might now be tempted to formulate the equation of motion of the bar as $F_k^+ - F_k^- = \rho h \ddot{u}_k$. However, this would not be a stable model since certain modes of nonzero displacements (other than rigid-body modes) could occur at zero stresses and zero energy (see Ref. 13). Therefore, it is necessary to assume that, in addition to the imbricate (regularly overlapping) elements of fixed length l, adjacent nodes are also connected

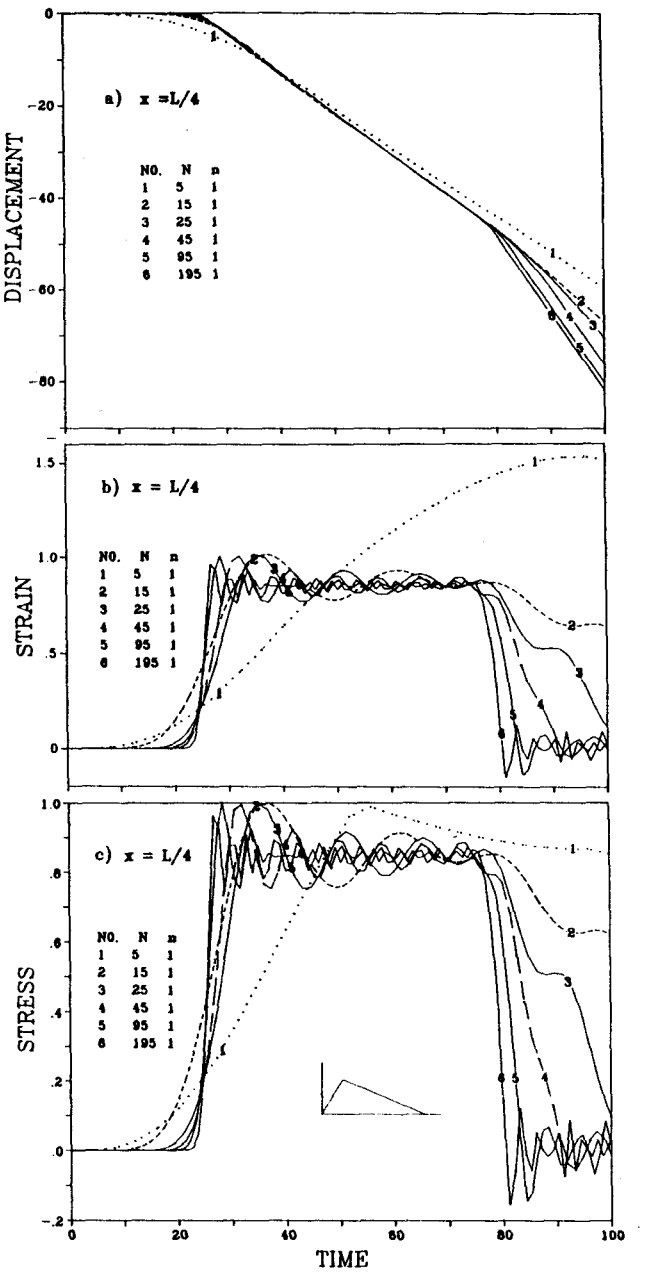

FIG. 3.—Results for Strain-Softening Local Continuum—Convergence of Time History

by regular finite elements of length h. Their cross section must equal c, so that the cross-section areas of all elements intersecting a given cross-section would add up to 1. The strains and stresses in these elements, called local, may be expresed as

$$\epsilon_k = \frac{1}{h}(u_{k+1} - u_k), \quad \epsilon_{k-1} = \frac{1}{h}(u_k - u_{k-1}) \quad \text{..... (8)}$$

$$\tau_k = E(\epsilon_k)\epsilon_k, \quad \tau_{k-1} = E(\epsilon_{k-1})\epsilon_{k-1} \quad \text{..... (9)}$$

and the nodal forces from these elements [Fig. 3(*d*)] are

$$f_k^+ = c\,\tau_k, \quad f_k^- = c\,\tau_{k-1} \quad \text{..... (10)}$$

Considering all mass to be lumped in the nodes, the equation of motion of node k is $F_k^+ - F_k^- + f_k^+ - f_k^- = \rho h \ddot{u}_k$ or

$$\frac{1-c}{n}\left[\bar{E}(\bar{\epsilon}_k)\frac{u_{k+n} - u_k}{l} - \bar{E}(\bar{\epsilon}_{k-n})\frac{u_k - u_{k-n}}{l}\right]$$

$$+ c\left[E(\epsilon_k)\frac{u_{k+1} - u_k}{h} - E(\epsilon_{k-1})\frac{u_k - u_{k-1}}{h}\right] = \rho h \ddot{u}_k \quad \text{..... (11)}$$

This may be rearranged as

$$\frac{1-c}{l^2}[\bar{E}(\bar{\epsilon}_k)(u_{k+n} - u_k) - \bar{E}(\bar{\epsilon}_{k-n})(u_k - u_{k-n})] + \frac{c}{h^2}[E(\epsilon_k)(u_{k+1} - u_k)$$

$$- E(\epsilon_{k-1})(u_k - u_{k-1})] = \rho \ddot{u}_k \quad \text{..... (12)}$$

which applies only at points x_k that lie at distances at least $l/2$ from the boundaries. For the special case of elastic materials, i.e., constant $\bar{E}$ and E, the equation simplifies as

$$(1-c)\bar{E}\frac{u_{k+n} - 2u_k + u_{k-n}}{l^2} + cE\frac{u_{k+1} - 2u_k + u_{k-1}}{h^2} = \rho \ddot{u}_k \quad \text{..... (13)}$$

The total stress S_k between nodes k and $k+1$ [Fig. 2(*c*)] is the sum of the forces in all imbricate elements bridging the segment $(k, k+1)$, plus the force from the local element $(k, k+1)$. Therefore

$$S_k = \frac{1-c}{n}\sum_{j=1}^{n}\sigma_{k+1-j} + c\tau_k \quad \text{..... (14)}$$

Continuum as Limiting Case

The continuum limit of Eq. 12 ($h \to 0$ at constant l) is now obvious:

$$\frac{1-c}{l^2}\left\{\bar{E}\left(x + \frac{l}{2}\right)[u(x+l) - u(x)] - \bar{E}\left(x - \frac{l}{2}\right)[u(x) - u(x-l)]\right\}$$

$$+ c\frac{\partial}{\partial x}\left[E(x)\frac{\partial u(x)}{\partial x}\right] = \rho\frac{\partial^2 u(x)}{\partial t^2} \quad \text{..... (15)}$$

and for the special case of elastic materials (constant $\bar{E}$ and E):

$$(1-c)\frac{\bar{E}}{l^2}[u(x+l) - 2u(x) + u(x-l)] + cE\frac{\partial^2 u(x)}{\partial x^2} = \rho\frac{\partial^2 u(x)}{\partial t^2} \quad \text{..... (16)}$$

Introducing the difference operator, D_x, as

$$D_x u(x) = \frac{1}{l}\left[u\left(x + \frac{l}{2}\right) - u\left(x - \frac{l}{2}\right)\right] \quad \text{..... (17)}$$

and omitting the arguments at $\bar{E}$ and E, we can write Eq. 15 more tersely as

$$(1-c)D_x[\bar{E}D_x u(x)] + c\frac{\partial}{\partial x}\left[E\frac{\partial u(x)}{\partial x}\right]$$

$$= \rho\frac{\partial^2 u(x)}{\partial t^2} \quad \left(\text{for} \quad \frac{l}{2} \le x \le L - \frac{l}{2}\right) \quad \text{..... (18)}$$

in which L = bar length, or as

$$(1-c)D_x\sigma(x) + c\frac{\partial}{\partial x}\tau(x) = \rho\frac{\partial^2 u(x)}{\partial t^2} \quad \text{..... (19)}$$

$$\text{with} \quad \sigma(x) = \bar{E}D_x u(x), \quad \tau(x) = E\frac{\partial}{\partial x}u(x) \quad \text{..... (20)}$$

Here τ may be called the local stress, and σ the broad-range stress. In contrast to $\bar{\epsilon}$, σ must be regarded strictly as the stress in the imbricate elements of fixed length l, and not as the mean of stresses within l. (This is why we do not write $\bar{\sigma}$ instead of σ.) In the continuum limit, every point is bridged by infinitely many imbricate (overlapping) elements, each one of them having an infinitely small cross section. It should also be noted that, in Eq. 19

$$D_x\sigma(x) = \frac{1}{l}\int_{-l/2}^{l/2}\frac{\partial\sigma(x+s)}{\partial s}ds = \frac{1}{l}\int_{x-l/2}^{x+l/2}\frac{\partial\sigma(x')}{\partial x'}dx'$$

$$= \frac{1}{l}\left[\sigma\left(x + \frac{l}{2}\right) - \sigma\left(x - \frac{l}{2}\right)\right] \quad \text{..... (21)}$$

i.e., $D_x\sigma(x)$ is the mean stress gradient although σ is not the mean stress.

The total stress, $S(x)$, is the resultant of all forces within the unit cross section of the bar. One cross section, x, cuts all the imbricate elements having their centers at $x + s$ such that $-l/2 \le s \le l/2$ [Fig. 2(*c*)]. Therefore

$$S(x) = (1-c)\bar{\sigma}(x) + c\tau(x) \quad \text{..... (22)}$$

$$\text{with} \quad \bar{\sigma}(x) = H\sigma(x) = \frac{1}{l}\int_{-l/2}^{l/2}\sigma(x+s)\,ds = \frac{1}{l}\int_{x-l/2}^{x+l/2}\sigma(x')\,dx' \quad \text{..... (23)}$$

in which H is an averaging operator. Eq. 22 is the limit of Eq. 14 for $n \to \infty$. The total stress, S, is the only stress that can be applied or controlled at the boundary; σ and τ are in fact hidden (internal) variables, directly unobservable. Note that $\bar{\sigma}(x)$ is the mean broad-range stress, and that the relation of $\bar{\sigma}$ to ϵ involves double averaging, i.e.,

$$\bar{\sigma} = H\bar{E}H\epsilon; \quad S = (1-c)H\bar{E}H\epsilon + cE\epsilon \quad \text{(24)}$$

Because $\partial(H\sigma)/\partial x = H(\partial\sigma/\partial x) = D_x\sigma$ and $D_x u = H\epsilon$, the use of S allows the continuum equation of motion (Eq. 19) to be written in the familiar form

$$\frac{\partial S(x)}{\partial x} = \rho\frac{\partial^2 u(x)}{\partial t^2} \quad \text{(25)}$$

One crucial aspect is the difference operator on stress, $D_x\sigma$, which is equivalent to averaging of the stress gradient. The salient property that gives rise to the difference operator on stress and distinguishes the present nonlocal continuum theory from the existing (classical) one is the fact that imbricated (regularly overlapping) elements interlink each point of the continuum with points at a finite distance, l [Fig. 2(*d*)], without being linked to the points lying in between. To emphasize this crucial aspect, the present continuum may be called the *imbricate continuum*.

By virtue of this imbricate structure, it is possible to introduce *two different* and independent stress-strain relations: the broad-range one, and the local one. The latter must not exhibit strain-softening, while the former may. This is an important aspect, and until it was adopted, computer simulations had not succeeded in producing convergent behavior and finite-size strain-softening zones.

The essential difference between the imbricate nonlocal continuum and the existing (classical) nonlocal continuum is the fact that the present continuum equation of motion (Eq. 20) has a difference operator, $D_x\sigma$ (or gradient averaging operator), where the classical nonlocal theory has a differential expression, $(\partial/\partial x)\sigma$. Accordingly, Eq. 19 has a double difference operator, $D_x\bar{E}D_x u$ (or double gradient averaging operator), where the classical nonlocal theory for the case of uniform weights, $\alpha(s)$, has a differential-difference operator $(\partial/\partial x)(ED_x u)$. The dichotomy of combining, in the classical nonlocal theory, a difference operator (or gradient averaging operator) for the displacement u with a differential operator for the stress σ appears to be one reason why a highly nonlinear behavior such as strain-softening cannot be modeled.

The operator $D_x\bar{E}D_x u$ leads in finite element approximation to a symmetric stiffness matrix (see Eq. 12), while the operator $\partial(ED_x u)/\partial x$ does not. The lack of symmetry in the classical nonlocal theory, which exists even if linear elasticity is assumed, is quite disturbing, and may be the cause of certain instabilities. Moreover, the nonsymmetry raises questions with regard to the laws of thermodynamics.

Alternative Formulations

The continuum equation of motion may also be written with the help of a weighted operator, $\bar{D}_x$, defined by

$$\bar{D}_x u(x) = \int_{-\infty}^{\infty}\frac{\partial u(x+s)}{\partial s}\alpha(s)ds \quad \text{(26)}$$

which has been used in the existing nonlocal continuum theory (compare Eq. 1). If we introduce the weighting function as

$$\alpha(s) = \frac{1-c}{l} + c\delta(s) \quad \text{for} \quad |s| \le \frac{l}{2}; \quad \alpha(s) = 0 \quad \text{for} \quad |s| > \frac{l}{2} \quad \text{(27)}$$

with $\delta(s)$ = Dirac delta function, we have

$$\bar{D}_x u(x) = (1-c)D_x u(x) + c\frac{\partial u(x)}{\partial x} = (1-c)H\epsilon(x) + c\epsilon(x) \quad \text{(28)}$$

in which D_x is the operator defined before by Eq. 17. Now, according to the existing nonlocal theory, the continuum equation of motion would be $(\partial/\partial x)E\bar{D}_x u(x) = \rho\partial^2 u(x)/\partial t^2$ (instead of Eq. 18). If elimination of nonsymmetry of the left-hand side of this equation is desired, one could assume a continuum equation of motion of the form

$$\bar{D}_x E\bar{D}_x u(x) = \rho\frac{\partial^2 u(x)}{\partial t^2} \quad \text{(29)}$$

For $\alpha(s)$ according to Eq. 27, Eq. 29 may be written as

$$(1-c)^2 D_x E D_x u(x) + c(1-c)\left[\frac{\partial}{\partial x}ED_x u(x) + D_x E\frac{\partial}{\partial x}u(x)\right] + c^2\frac{\partial}{\partial x}E\frac{\partial u(x)}{\partial x} = \rho\frac{\partial^2 u(x)}{\partial t^2} \quad \text{(30)}$$

This equation, however, is not equivalent to Eq. 18, and so the discrete approximation of Eq. 29 or 30 does not consist of a system of imbricated finite elements and appears to be more involved. Eq. 30 may be also written in the form of Eq. 25, with

$$S = (1-c)^2 HEH\epsilon + c(1-c)(EH\epsilon + HE\epsilon) + c^2 E\epsilon = \bar{H}E\bar{H}\epsilon \quad \text{(31)}$$

in which $\bar{H}\epsilon = \bar{D}_x u$ and $\bar{H}$ is a weighted averaging operator, defined by Eq. 1. Again, Eq. 31 is not equivalent to Eq. 24 obtained from the imbricate discrete model.

Since Eq. 30 does not permit the imbricate element discretization, there is no objection to using various other weighting functions in Eq. 26; e.g., the error function (normal or Gaussian distribution), for which $\alpha(s) = (2\pi)^{-1/2}l^{-1}\exp(-s^2/2l^2)$, or the bilateral exponential distribution, for which $\alpha(s) = (2l)^{-1}\exp(-|s|/l)$. For both of these functions, the classic elastic nonlocal continuum is stable even without superimposing a delta function (13).

The nonsymmetry of the classical nonlocal theory was first noted by Belytschko (22). Writing the discrete stress-strain relation as $\mathbf{S} = E\,\bar{\boldsymbol{\epsilon}} = E\mathbf{H}\boldsymbol{\epsilon}$ in which $\boldsymbol{\epsilon}$ and $\mathbf{S}$ are the column matrices of strains and (total) stresses in all elements and $\mathbf{H}$ is a square matrix that corresponds to averaging according to Eq. 23 (with uniform weight α), he noted that the resulting stiffness matrix is not symmetric, and proposed the modification $\mathbf{S} = \mathbf{H}^T E\mathbf{H}\boldsymbol{\epsilon}$, the similarity of which (to Eqs. 31 and 24) is obvious (although different E and $\bar{E}$ cannot be distinguished here). Another symmetrizing possibility, equivalent to $\mathbf{H}^{-1}\mathbf{S} = E\mathbf{H}\boldsymbol{\epsilon}$, was independently suggested by Bažant, who was also the first to introduce the imbricate discrete model, replace $\partial\sigma/\partial x$ in the continuum equation of motion by an averaging operator on the stress gradient, and note the aforementioned instabilities and the possibility of stabilization by an addition-

al local term (i.e., $c > 0$) for which a different E, i.e., a different nonsoftening stress-strain relation, is used (6,7,8).

Stability of Continuum

We still need to justify the presence of the local term with $\partial u/\partial x$ in Eqs. 18 or 15. Let us consider the elastic case, i.e., constant E and $\bar{E}$, and (similarly to Ref. 13) seek static solutions of the form $u = Ae^{i\kappa x}$, in which A and κ are real constants, $\kappa > 0$, and i = imaginary units. Substituting this into Eq. 16 with $\partial^2 u/\partial t^2 = 0$, we obtain for $A \neq 0$ the condition $(1 - c)\bar{E}_t(e^{i\kappa l} - 2 + e^{-i\kappa l}) = cE\kappa^2 l^2$. Its imaginary part is automatically satisfied, and its real part yields the condition

$$2(1 - c)\bar{E}_t(1 - \cos \kappa l) + cE(\kappa l)^2 = 0 \quad \ldots\ldots\ldots\ldots\ldots\ldots\ldots\ldots \quad (32)$$

When $c = 1$, which is the case of local continuum, this equation is never satisfied (for $\kappa > 0$), which means that $A = 0$, i.e., the local continuum is stable. When $c = 0$, we have $1 - \cos \kappa l = 0$; this may be satisfied for $\kappa = 2n\pi/l$ (n = 1, 2, 3, ...), which means that periodic solutions of wavelength l/n and arbitrary amplitude A (13) are possible. Therefore, the imbricate nonlocal continuum with $c = 0$ is unstable, and the stability requirement is $c > 0$, because then Eq. 31 has no nonzero solution κ. For this reason, the local term had to be included.

It is interesting to compare this with the corresponding static elastic solution for the existing nonlocal continuum theory, for which $\partial(E\bar{D}_x u)/\partial x = 0$. Introducing again $u = Ae^{i\kappa x}$, we then obtain, instead of Eq. 31, the condition $cEy + (1 - c)\bar{E} \sin y = 0$ where $y = \kappa l/2$. This condition has no positive solution κ if $c > 0.178465\ \bar{E}/E$ (13). This stability condition is more stringent than the one for the present theory (Eq. 32), which suggests that the symmetry has a stabilizing influence.

It is further interesting to check the static stability condition for Eq. 30. In this case, the same substitution as before for u leads to the condition

$$1 - \cos \kappa l + \frac{c}{1 - c}\kappa l \sin \kappa l + \frac{1}{2}\left(\frac{c}{1 - c}\right)^2 (\kappa l)^2 = 0 \quad \ldots\ldots\ldots\ldots\ldots\ldots \quad (33)$$

One can now show that no solutions with $\kappa > 0$ exist for $c > 0$, and that $c = 0$ leads to instability. So the stability condition is again $c > 0$. However, the minimum of the left-hand side of Eq. 33 approaches 0 as κ^2 (quadratically), while that of Eq. 32 approaches 0 as κ (linearly). Thus, for small c, the formulation based on Eq. 30 would exhibit more noise than the imbricate one.

Strain-Softening Law and Numerical Studies

Strain-softening is an overall property of the representative volume, not a point property of a continuum. As already mentioned, strain-softening is always caused by some randomly dispersed, highly localized defects, such as microcracks or voids. If they are treated as point defects, and if it is assumed that the number of such defects within a finite volume is finite, then the probability of encountering a defect at a randomly chosen point is zero, while the probability of encountering a defect in the representative volume of size l is finite and large. Thus, although

the local stress-strain relation $\tau = E(\epsilon)\epsilon$ may exhibit plasticity, it may *not* exhibit strain-softening, i.e., the local tangent modulus, $E_t = E + \epsilon\, dE/d\epsilon$, may not be negative. Strain-softening can be exhibited only by broad-range stresses, σ, and not by local stresses, τ. Positiveness of E_t is also required by stability, as numerical calculations confirm.

For numerical examples, we consider the bilinear stress-strain diagrams shown in Fig. 2(*e*). The broad-range stress-strain diagram has an elastic (straight) rising branch of slope E_0 up to peak stress σ_p corresponding to strain ϵ_p, then a straight declining (strain-softening) branch of negative slope $\bar{E}_t$, and finally, a nearly horizontal tail of a very small positive slope $\bar{E}_f$ (a zero slope might be inconvenient for numerical computations). The local stress-strain diagram is elastic up to strain ϵ_f, with a positive slope E_0, and beyond ϵ_f, it is plastic, i.e., nearly horizontal, with a very small positive slope, $\bar{E}_f$. For the tail portion of the broad-range diagram two types were considered [Fig 2(*e*)]: Type I, in which the broad-range strain-softening dips below the strain axis so that the tail of the total stress diagram [Fig. 2(*e*)] would be approximately zero, as after full fracturing; and Type II, in which the broad-range strain-softening terminates at zero stress [Fig. 2(*e*)] so that the tail of the total-stress diagram ends with a plateau of finite stress. Type II is probably more reasonable physically, but Type I is a convenient way to obtain full strain-softening (full fracturing) of the material. (If the broad-range stress-strain diagram were not allowed to dip below the strain axis [Fig. 2(*e*)], then a continuation of strain-softening beyond strain ϵ_f could be modeled by using a hierarchy of broad-range stresses corresponding to different layers of imbricate elements with different lengths $l = l_1, l_2, \ldots$; this would, however, be too complex.)

For unloading and reloading, we assume that a positive slope, $\bar{E}_u$ or E_u, always applies [Fig. 2(*e*)]. In the present computations it was assumed, for the sake of simplicity, that $\bar{E}_u$ and E_u are constant for both the broad-range and local stresses. Negative $\Delta\bar{\epsilon}$ or $\Delta\epsilon$ means unloading, while nonnegative $\Delta\bar{\epsilon}$ or $\Delta\epsilon$ is either a virgin loading or reloading, depending on whether the strain is equal or less than the previous maximum of strain. If reloading returns to the last previous maximum strain, the virgin stress-strain diagram is again followed until the strain increment becomes negative. Note that it is possible to have loading for the broad-range stress and unloading for the local stress at the same time.

For numerical conputations, the material properties are specified as $E_0 = \bar{E}_0 = 1$, $\epsilon_p = 1$, $\epsilon_f = 5$, $E_f = \bar{E}_f = 0.001$, and $l = L/5$, in which L = length of bar [Fig. 2(*b*)]. For Type I softening [Fig. 2(*e*)], σ at $\epsilon = \epsilon_f$ was considered as 0; and for Type II softening, it was considered as $E_0\epsilon_f c$. These values then yield $\bar{E}_t$.

The length, L, of the one-dimensional bar is subdivided into N elements of length $h = L/N$ with $N_n = N + 1$ nodes [Fig. 2(*b*)]. The velocities c_1 and c_2 for both ends of the bar ($x = 0$ and $x = L$) are prescribed for all time steps. The arrangement of the local elements is shown in Fig. 2(*b*).

A question arises with regard to the treatment of the boundaries for the imbricate (overlapping) elements. For the sake of simplicity, those elements which would overlap beyond the boundary are shortened so as to terminate at the boundary node to which they are attached [Fig.

2(c)]. Thus, the first and last imbricate elements (from $k = 1$ to $k = 2$, and from $k = M - 1$ to $k = M$) are of length h and are equivalent to the local elements.

The computation is carried out in small time steps Δt using the explicit algorithm which follows, in which subscripts $r = 1, 2, \ldots N_t$ refer to discrete times, t_r; subscripts $r \pm 1/2$ to times $t_r \pm \Delta t/2$; subscripts $i = 1, 2, \ldots, N_e$ to element numbers; and subscripts $k = 1, 2, \ldots, N_n$ to node numbers.

1. Read h, l, Δt, N_t, N_n, N_e, $\bar{N}_e$, c_1, c_2, and constitutive parameters; generate all t_r. Generate arrays $K(i)$, $M(i)$, $l_e(i)$, $\bar{K}(i)$, $\bar{M}(i)$, $\bar{l}_e(i)$ giving the numbers of the left and right node of the ith local or imbricate element, and its length. Initialize for $r = 1$: $v_{k,r-1/2}$, $u_{k,r}$, $\tau_{k,r}$, $\sigma_{k,r}$, max ϵ_k, max $\bar{\epsilon}_k$, $\tau_{\max\epsilon,k}$, $\sigma_{\max\epsilon,k}$ all as zero, for all k.

2. DO 11, $r = 1, \ldots, N_t$ (time steps).

3. $v_{1,r} = -c_1$, $v_{N_n,r} = c_1$. Initialize $F_k = 0$, $f_k = 0$ for all nodes $k = 2, 3, \ldots, N_n - 1$.

4. DO 6, $i = 1, \ldots, N_e$ (local elements).

5. $k = K(i)$, $m = M(i)$; $\Delta\epsilon_{i,r} = (v_{m,r} - v_{k,r})\Delta t/l_e(i)$, $\epsilon_{i,r} = \epsilon_{i,r-1} + \Delta\epsilon_{i,r}$. CALL subroutine MODL ($\Delta\epsilon$, ϵ, max ϵ, $\tau_{\max\epsilon}$) which determines from the foregoing arguments the tangential moduli $E_{i,r}$ of the local elements.

6. $\tau_{i,r} = \tau_{i,r-1} + E_{i,r}\Delta\epsilon_{i,r}$. If $\Delta\epsilon_{i,r} > 0$: max $\epsilon_i = \epsilon_{i,r}$ and $\tau_{\max\epsilon,i} = \tau_{i,r}$. Accumulate nodal forces: $f_k \leftarrow f_k - c\tau_{i,r}$, $f_m \leftarrow f_m + c\tau_{i,r}$.

7. DO 9, $i = 1, \ldots, \bar{N}_e$ (imbricate elements).

8. $k = \bar{K}(i)$, $m = \bar{M}(i)$; $\Delta\bar{\epsilon}_{i,r} = (v_{m,r} - v_{k,r})\Delta t/\bar{l}_e(i)$, $\bar{\epsilon}_{i,r} = \bar{\epsilon}_{i,r-1} + \Delta\bar{\epsilon}_{i,r}$. CALL subroutine MODB ($\Delta\bar{\epsilon}$, $\bar{\epsilon}$, max $\bar{\epsilon}$, $\sigma_{\max\epsilon}$) which determines the tangential moduli $\bar{E}_{i,r}$ of the imbricate elements.

9. $\sigma_{i,r} = \sigma_{i,r-1} + \bar{E}_{ir}\Delta\bar{\epsilon}_{i,r}$. If $\Delta\bar{\epsilon}_{i,r} > 0$: max $\bar{\epsilon}_i = \bar{\epsilon}_{i,r}$ and $\sigma_{\max\epsilon,i} = \sigma_{i,r}$. Accumulate nodal forces $F_k \leftarrow F_k - (1 - c)\sigma_{i,r}$ (left node), $F_m \leftarrow F_m + (1 - c)\sigma_{i,r}$ (right node).

10. DO 11, $k = 2, \ldots, N_n - 1$ (all interior nodes).

11. $v_{k,r+1/2} = v_{k,r-1/2} + (F_k + f_k)\Delta t/(\rho h)$, $u_{k,r+1} = u_{k,r} + \Delta t v_{k,r+1/2}$.

The time step Δt must be within the limit for numerical stability. One limit for the imbricate elements, and another for the local elements may be considered. The latter, which is smaller and decides, is $\Delta t \leq h/v$, in which $v = \sqrt{(E_0/\rho)}$. The time step $\Delta t = 0.2\, h/v$ was used.

As the initial condition, the bar is assumed to be at rest at $t = 0$. As the boundary conditions, the ends of the bar of length L are assumed to move at constant velocities, c_1 and c_2, away from the bar; $c_1 = -c_2$. For the usual elastic continuum, this loading generates two tensile step waves of constant strain $\epsilon = c_1$, propagating toward each other. As they meet at the center of the bar, the strain is instantly doubled.

To study a strain-softening imbricate continuum, we select such boundary velocity c that the strain of the inward wave is slightly below the limit of proportionality, ϵ_p; $c_1 = 0.85\epsilon_p$ was used. Thus, the inward waves are elastic and run essentially at wave velocity $v = \sqrt{(E_0/\rho)}$, except for wave dispersion due to length l of the imbricate elements, which blurs the wave front more than is seen for the local elastic material, i.e., for $l = h$. (This blurring occurs even for the nonlocal continuum, not just for the discrete model.) At approximately the time $t = L/2v$, the wave-

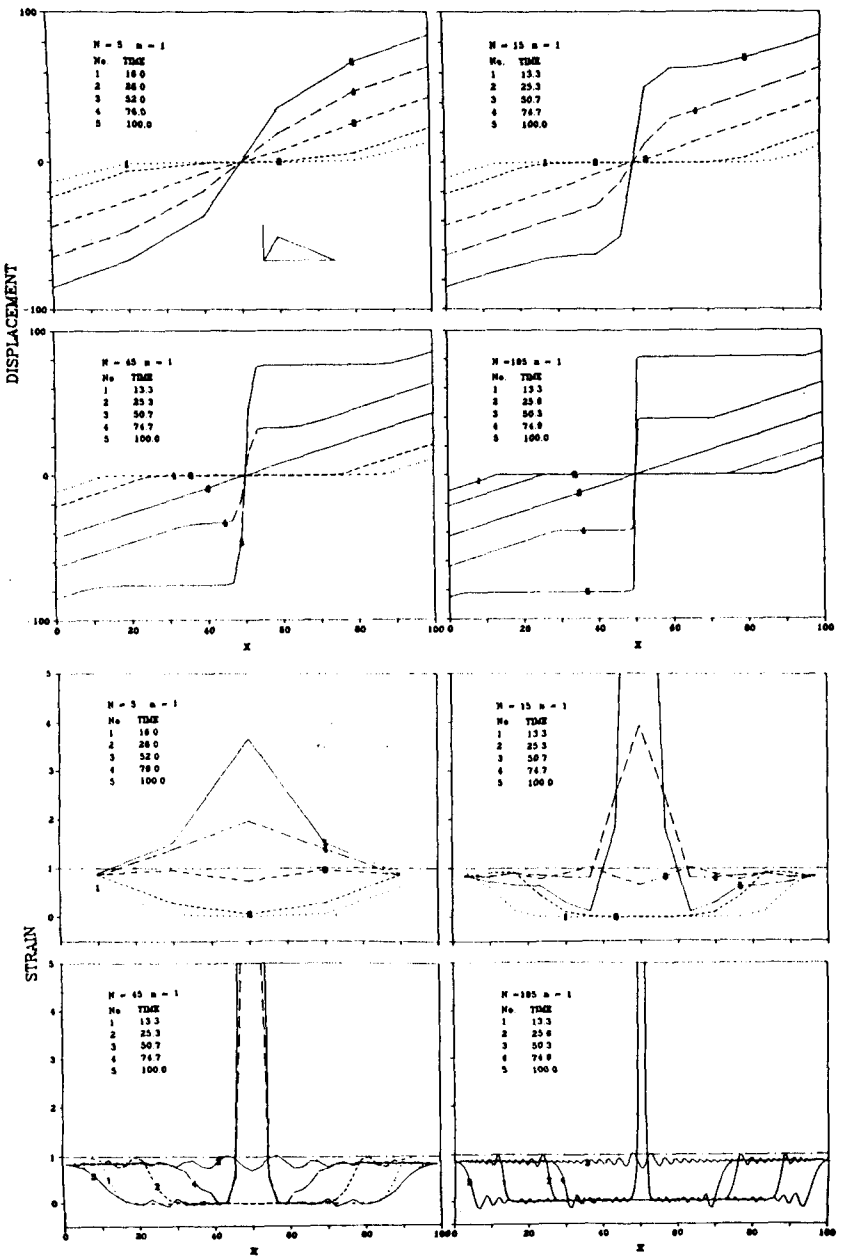

FIG. 4.—Results for Local Strain-Softening Continuum—Spatial Distributions at Various Times for Increasingly Refined Mesh

fronts meet at the center of the bar. The strain then rapidly exceeds ϵ_p and enters the strain-softening range.

First it has been checked that for the case in which $c = 1$ and $\bar{E} = \text{const.}$, as well as for the case in which $\bar{E} = E = \text{constant}$ and $c \neq 1$, the response converges to the exact solution for the usual local elastic continuum as h is decreased. Then, it has been checked that for $c = 1$ and a hardening plastic stress-strain relation, the response converges as h is decreased to the known plastic wave solution.

Further, it has been checked that for $c = 0$ and strain-softening local material properties [of Type I, Fig. 2(*e*)], the response (Figs. 3–4) converges for decreasing h to the exact solution which has been recently worked out (9). This solution indicates that the strain-softening region at the bar center remains of zero length; the strain instantly drops to

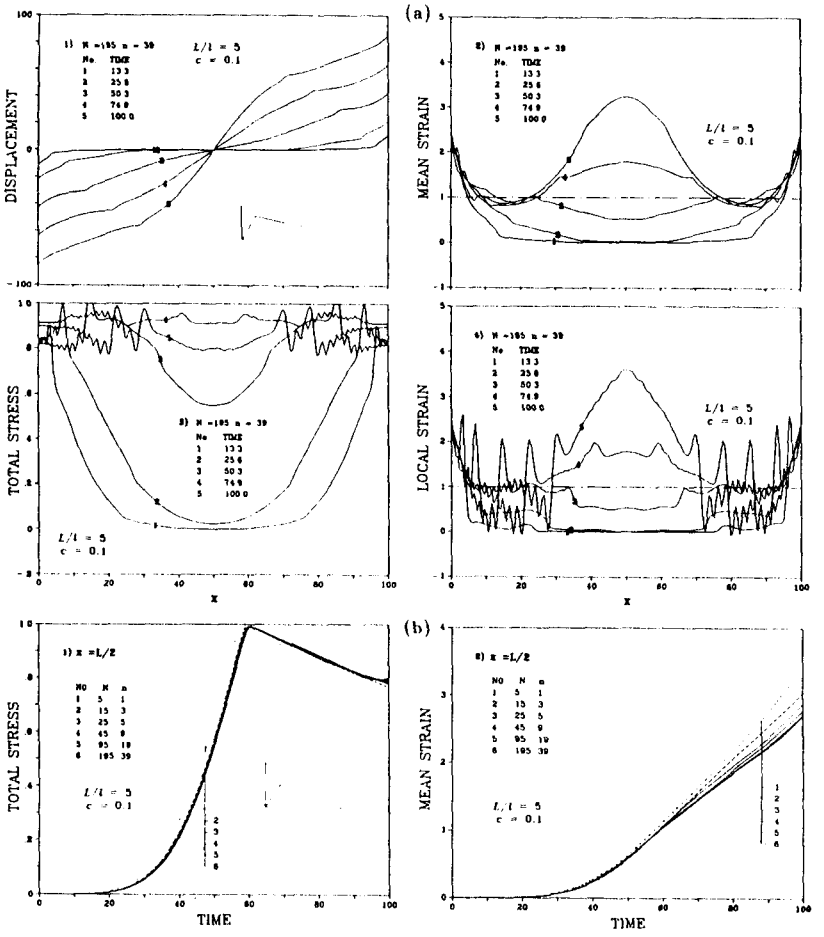

FIG. 5.—Results for Partially Strain-Softening Imbricate Continuum: (*a*) Spatial Distributions at Various Times for the Finest Mesh; (*b*) Convergence of Time Histories at Mesh Refinement

zero as soon as the wavefronts meet, and an outward unloading wave of strain step $(-c_1/v)$ is reflected from the boundary of the strain-softening region, canceling the strain of the inward wave (9). As is seen from Figs. 3 and 4, the numerical solution (for $l = h$) converges at decreasing h to this exact solution. (This invalidates the claims in recent debates that convergence cannot occur.) The convergence is slow at the wavefront, but this is typical whenever waves with step wavefronts are considered.

Now consider convergence at constant l and decreasing h for the strain-softening imbricate continuum—the goal of this work. Empirically, it has been found that the smallest value of coefficient c for which the calculated response appears stable and free of noise is roughly $c = 0.1$. This value has been used in all computations. The calculated responses for successively refined subdivisions of bar length L ($N = 5$, 15, 45 and 195) are plotted in Fig. 5 for partial strain-softening [Fig. 2(*e*), Type II] and in Figs. 6–9 for full strain-softening [Fig. 2(*e*), Type I]. We see that the responses exhibit a strain-softening region of a finite length, and converge as the subdivision of the bar length is refined. With this, our goal is achieved.

We may also note (Figs. 6, 8) that the length of the strain-softening region quickly grows after time $t = L/2v$, until it reaches a characteristic constant value roughly equal to $2l$. (This fact lends support to the crack band model.) By contrast, for the usual, local continuum that exhibits strain-softening, the size of the strain-softening region cannot grow and remains zero (9) (Fig. 4). (The length of the strain-softening region in the imbricate continuum could be made to grow beyond $2l$ only by other

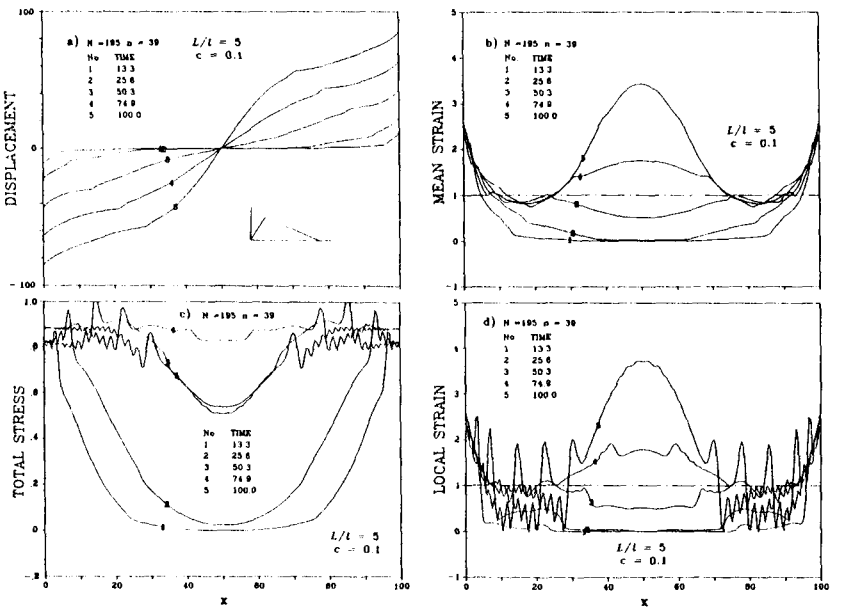

FIG. 6.—Results for Fully Strain-Softening Imbricate Continuum, for Finest Mesh

influences, such as embedded reinforcing bars or, in two or three dimensions, by the restraining effect of an adjacent compressed region, as in bending.)

For applications to the dynamics of concrete structures, e.g., resistance to impact, blast or earthquake, the calculated value of total energy absorption W in the bar is of great interest. Assuming straight-line unloading with modulus E_u, the enrgy consumed during $\Delta t = t_{r+1} - t_r$ per unit length of one imbricate element is (see Fig. 10):

$$\Delta \bar{W}_r = \frac{1}{2}\left[\frac{\sigma_r^2}{E_{u,r}} - \frac{\sigma_{r+1}^2}{E_{u,r+1}} + (\sigma_r + \sigma_{r+1})\Delta\epsilon\right] \quad \text{for} \quad \text{any } E_u\text{-variation} \ldots\ldots (34)$$

$$\Delta \bar{W}_r = \frac{1}{2}(\sigma_r + \sigma_{r+1})\left(\Delta\epsilon - \frac{\Delta\sigma}{E_u}\right) \quad \text{for} \quad \text{constant } E_u \ldots\ldots\ldots\ldots (35)$$

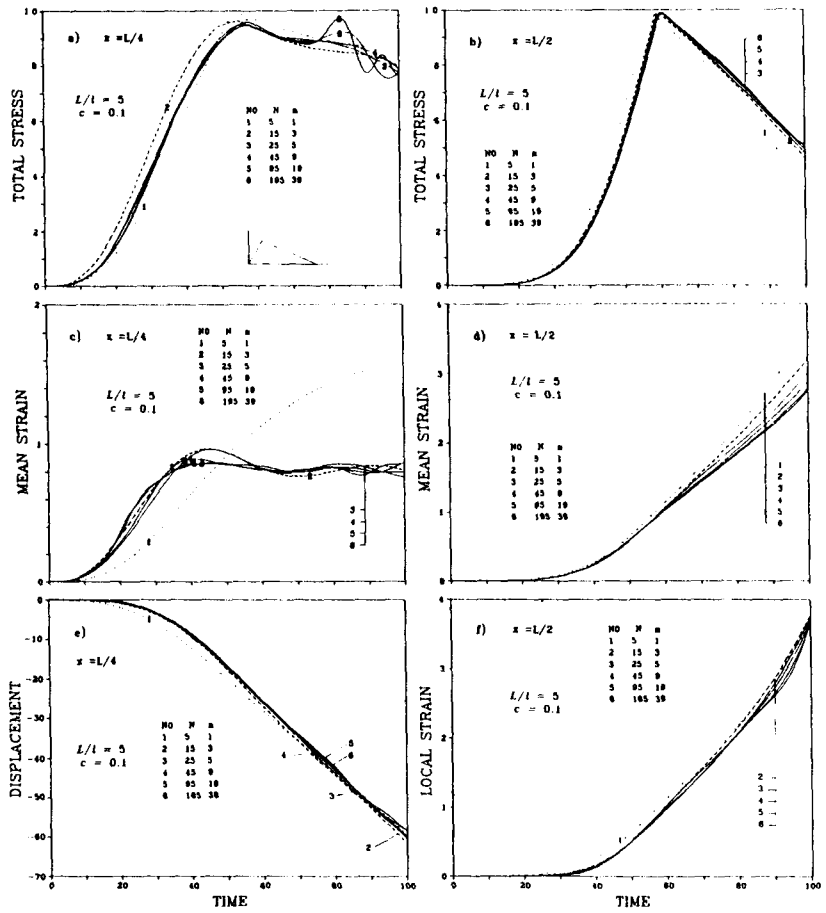

FIG. 7.—Results for Fully Strain-Softening Imbricate Continuum—Convergence of Time Histories at Mesh Refinement

$$\Delta \bar{W}_r = \frac{1}{2}(\sigma, \Delta\bar{\epsilon} - \bar{\epsilon}, \Delta\sigma) \quad \text{for} \quad E_u = \frac{\sigma}{\epsilon}\,(\text{secant}) \ldots\ldots\ldots\ldots\ldots\ldots (36)$$

and the total energy consumption is

$$W = \sum_r \sum_i \frac{1-c}{n}\, \bar{l}_e(i)\, \Delta \bar{W}_r(i) \ldots\ldots\ldots\ldots\ldots\ldots\ldots\ldots\ldots\ldots\ldots (37)$$

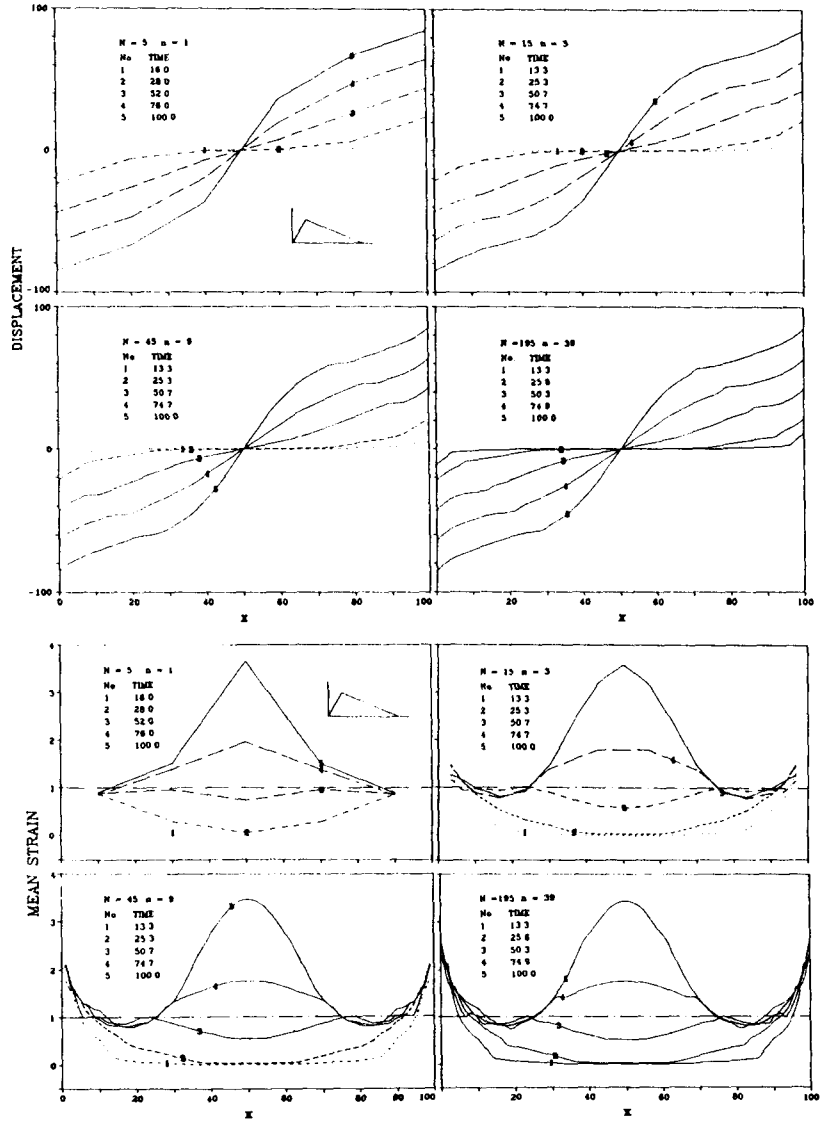

FIG. 8.—Results for Fully Strain-Softening Imbricate Continuum—Convergence of Spatial Distributions at Various Times with Mesh Refinement

in which $\bar{l}_e(i)$ = length of imbricate element No. i. Note that this expression gives $\Delta\bar{W}_r = 0$ for elastic deformations, and that it may be used even for unloading and reloading. At full softening, $\Sigma\,\Delta\bar{W}_r$ always equals the total area under the stress-strain diagram, regardless of strain history.

For the present solution (E_u = const.), the calculated W is plotted in Fig. 10 against the number, N, of subdivisions. Note that for the local continuum ($l = h$), W approaches 0 as $h \to 0$ and, therefore, no energy is consumed at all, which agrees with the exact solution in Ref. 9 but is

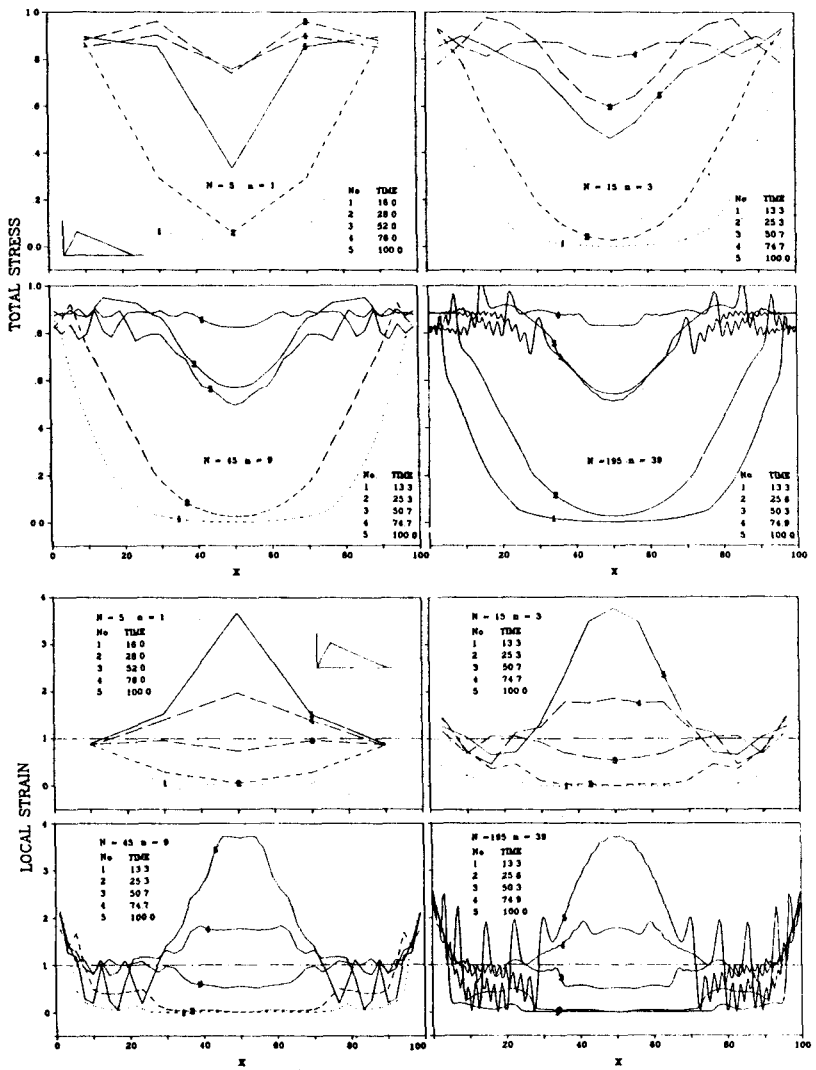

FIG. 9.—Fully Strain-Softening Imbricate Continuum—Further Results on Convergence of Spatial Distributions with Mesh Refinement

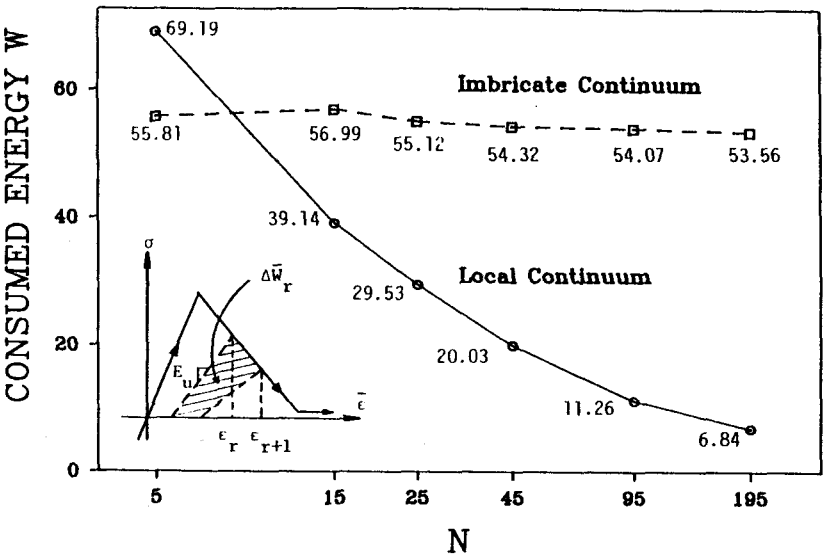

FIG. 10.—Energy Dissipated by Damage Due to Strain Softening

unrealistic from an engineer's viewpoint. For the imbricate continuum with $l = L/5$ = const., W converges to a finite value as $h \to 0$ (see Fig. 10), which is satisfactory from an engineer's viewpoint. Note that, if no energy is consumed within boundary segments of length l, the continuum limit is

$$W(t_1) = \int_0^{t_1}\int_0^{L} \frac{1-c}{2}\left\{d\left[\frac{\sigma^2(x)}{E_u}\right] + \sigma(x)d\epsilon(x)\right\} dx\,dt \quad \ldots\ldots\ldots\ldots\ldots\ldots \quad (38)$$

Conclusions

1. Stable strain-softening distributed over finite-size regions can be modeled by means of a new type of nonlocal continuum which may be called the imbricate continuum. This continuum is the limiting case (for vanishing mesh size) of a finite element system consisting of imbricated (regularly overlapping) elements which have a fixed characteristic length, l, that is kept constant as the mesh is refined, and a cross section which is reduced with the mesh size. The imbricate elements bridge all nodes within length l, while each node of the mesh is connected to some imbricate element. For stability reasons, the system of imbricate elements is overlaid by a system of ordinary elements that connect one node to the next and are refined if the mesh is refined.

2. The imbricate nonlocal continuum can be derived from the hypothesis that the stress depends on the change of distance between any pair of points lying at a certain characteristic distance, l, that is a material property. Equivalently, it can be postulated that the stress depends on the average of the strains within such a distance. In contrast to the existing (classical) nonlocal continuum theory, the averaging must be ap-

plied not only to the strains but also to the stress gradients. This is also necessary in order to obtain symmetric operators in the continuum equation of motion (or equilibrium), and symmetric finite element stiffness matrices.

3. In the existing (classical) nonlocal continuum theory, the operators in the continuum equation of motion are nonsymmetric (because the gradient operator is mixed with the gradient averaging operator). Consequently, the associated finite element stiffness matrices are nonsymmetric, too (even if the material is elastic).

4. Two types of stress must be distinguished—the broad range stress and the local stress—and the constitutive relation for each one of them must be different: the broad range one *with* strain-softening, and the local one *without* strain-softening.

5. Stability of the continuum, as well as numerical stability of an explicit time-step algorithm, can be achieved despite strain-softening. The numerical solution converges as the mesh size is refined in terms of energy as well as response histories and profiles. A finite energy is dissipated by failure due to strain-softening.

Acknowledgment

Financial support under AFOSR Grant No. 83-0009 to Northwestern University is gratefully acknowledged. Mary Hill is thanked for her superb secretarial assistance.

Appendix.—References

1. Bažant, Z. P., "Instability, Ductility and Size Effect in Strain-Softening Concrete," *Journal of the Engineering Mechanics Division*, ASCE, Vol. 102, No. EM2, 1976, pp. 331–344; discussions Vol. 103, pp. 357–358, 775–777, Vol. 104, pp. 501–502.
2. Bažant, Z. P., "Work Inequalities for Plastic Fracturing Materials," *International Journal of Solids and Structures*, Vol. 16, 1980, pp. 873–901.
3. Bažant, Z. P., "Crack Band Model for Fracture of Geomaterials," Proceedings of the 4th International Conference on Numerical Methods in Geomechanics, Z. Eisenstein, ed., Edmonton, Canada, Vol. 3, 1982, pp. 1137–1152.
4. Bažant, Z. P., "Size Effect in Blunt Fracture: Concrete, Rock, Metal," *Journal of Engineering Mechanics*, ASCE, Vol. 110, No. 4, 1984, pp. 518–535.
5. Bažant, Z. P., "Mechanics of Fracture and Progressive Cracking in Concrete Structures," *Fracture Mechanics Applied to Concrete Structures*, G. C. Sih, ed., Chapt. 7, Martinus Nijhoff Publishers V.B., The Hague, The Netherlands, 1984.
6. Bažant, Z. P., "Fracture in Concrete and Reinforced Concrete," *Mechanics of Geomaterials, Rocks, Concretes, Soils*, J. Wiley & Sons, Z. P. Bažant, ed., London, England (in press).
7. Bažant, Z. P., "Numerical Simulation of Progressive Fracture in Concrete Structures: Recent Developments," Proceedings of the Sept., 1984, International Conference, Computer-Aided Analysis and Design of Concrete Structures, held in Split, Yugoslavia, E. Hinton, R. Owen, and F. Damjanić, eds., University of Wales, Swansea, United Kingdom, Pineridge Press, Swansea, pp. 1–18.
8. Bažant, Z. P., "Imbricate Continuum and Progressive Fracturing of Concrete and Geomaterials," Proceedings of the Oct., 1984, International Symposium on Progress in Structural Analysis, commemorating the centenary of A. Castigliano's death, held at Politecnico di Torino, Meccanicca, Italy, Vol. 19, 1984, pp. 86–93.

9. Bažant, Z. P., and Belytschko, T. B., "Wave Propagation in Strain-Softening Bar: Exact Solution," *Report No. 83-10/401w*, Center for Concrete and Geomaterials, Northwestern University, Evanston, Ill., Oct., 1983; also *Journal of Engineering Mechanics*, ASCE, in press.
10. Bažant, Z. P., and Cedolin, L., "Fracture Mechanics of Reinforced Concrete," *Journal of the Engineering Mechanics Division*, ASCE, Vol. 106, No. EM6, Dec., 1980, pp. 1287–1306; Discussion and Closure, Vol. 108, 1982, pp. 464–471.
11. Bažant, Z. P., and Cedolin, L., "Blunt Crack Band Propagation in Finite Element Analysis," *Journal of the Engineering Mechanics Division*, ASCE, Vol. 105, No. EM2, Apr., 1979, pp. 297–315.
12. Bažant, Z. P., and Cedolin, L., "Finite Element Modeling of Crack Band Propagation," *Journal of Structural Engineering*, ASCE, Vol. 108, No. ST2, Feb., 1982, pp. 69–92.
13. Bažant, Z. P., and Chang, T. P., "Instability of Nonlocal Continuum and Strain Averaging," *Report No. 83-11/401i*, Center for Concrete and Geomaterials, Northwestern University, Evanston, Ill., Nov., 1983; also *Journal of Engineering Mechanics*, ASCE, Vol. 110, No. 10, Oct., 1984, pp. 1441–1450.
14. Bažant, Z. P., Chang, T. P., and Belytschko, T. B., "Continuum Theory for Strain-Softening," *Report No. 83-11/428c*, Center for Concrete and Geomaterials, Northwestern University, Evanston, Ill., Nov., 1983.
15. Bažant, Z. P., and Gambarova, P., "Crack Shear in Concrete: Crack Band Model," *Journal of Structural Engineering*, ASCE, Vol. 110, No. 9, Sept., 1984, pp. 2015–2035.
16. Bažant, Z. P., and Kim, J. K., "Size Effect in Shear Failure of Longitudinally Reinforced Beams," *American Concrete Institute Journal*, Vol. 81, No. 5, Sept.–Oct., 1984, pp. 456–468.
17. Bažant, Z. P., and Oh, B. H., "Crack Band Theory for Fracture of Concrete," *Materials and Structures*, RILEM, Paris, France, Vol. 16, 1983, pp. 155–177.
18. Bažant, Z. P., and Oh, B. H., "Deformations of Progressively Cracking Reinforced Concrete Beams," *American Concrete Institute Journal*, Vol. 81, May–June, 1984, pp. 268–278.
19. Bažant, Z. P., and Oh, B. H., "Rock Fracture via Strain-Softening Finite Elements," *Journal of Engineering Mechanics*, ASCE, Vol. 110, No. 7, July, 1984, pp. 1015–1035.
20. Bažant, Z. P., and Panula, L., "Statistical Stability Effects in Concrete Failure," *Journal of the Engineering Mechanics Division*, ASCE, Vol. 104, 1978, pp. 1195–1212.
21. Bažant, Z. P., Pfeiffer, P., and Marchertas, A. H., "Blunt Crack Band Propagation in Finite Element Analysis of Concrete Structures," *Transactions*, 7th International Conference on Structural Mechanics in Reactor Technology, SMiRT7, Chicago, Ill., Aug., 1983, Vol. 4, *Paper H5/2*, North-Holland Publishing Co., Amsterdam, The Netherlands, pp. 227–234.
22. Belytschko, T. B., Bažant, Z. P., and Hyun, Y., "Nonlocal Continuum Theories and Finite Elements," *Report No. 84-1/428n*, Center for Concrete and Geomaterials, Northwestern University, Evanston Ill., Jan., 1984.
23. Beran, M. J., and McCoy, J. J., "Mean Field Variations in a Statistical Sample of Heterogeneous Linearly Elastic Solids," *International Journal of Solids and Structures*, Vol. 6, 1970, pp. 1035–1054.
24. Bergan, P. G., "Numerical Modeling," Record of Discussions, *Mechanics of Geomaterials: Rocks, Concretes, Soils*, Z. P. Bažant, ed., Proceedings of the Sept., 1983, IUTAM W. Prager Symposium, held at Northwestern University, Evanston, Ill., J. Wiley and Sons, London, England (in press).
25. Burt, W. J., and Dougill, J. W., "Progressive Failure in a Model of Heterogeneous Medium," *Journal of the Engineering Mechanics Division*, ASCE, Vol. 103, No. EM3, June, 1977, pp. 365–376.
26. Cedolin, L., and Bažant, Z. P., "Effect of Finite Element Choice in Blunt Crack Band Analysis," *Computer Methods in Applied Mechanics and Engineering*, Vol. 24, No. 3, Dec., 1980, pp. 305–316.

27. Christensen, J., and Willam, K., "Finite Element Analysis of Concrete Failure in Shear," Proceedings of the Symposium on the Interaction of Non-Nuclear Munitions with Structures, U.S. Air Force Academy, Colorado Springs, May, 1983, pp. 101–106.
28. Darvall, P. L., "Critical Softening of Hinges in Indeterminate Beams and Portal Frames," *Civil Engineering Transactions*, Institution of Civil Engineers, Australia, 1983, pp. 199–209.
29. Darwall, P. LeP., "Shakedown with Softening in Reinforced Concrete Beams," *Report*, Monash University, Clayton, Victoria, Australia, 1983; also *Materials and Structures*, Paris, France (in press).
30. Eringen, A. C., "Nonlocal Polar Elastic Continua," *International Journal of Engineering Science*, Vol. 10, 1972, pp. 1–16.
31. Eringen, A. C., and Ari, N., "Nonlocal Stress Field at Griffith Crack," *Crystal Lattice Defects and Amorphous Materials*, Vol. 10, 1983, pp. 33–38.
32. Eringen, A. C., and Edelen, D. G. B., "On Nonlocal Elasticity," *International Journal of Engineering Science*, Vol. 10, 1972, pp. 233–248.
33. Hadamard, J., *Leçons sur la propagation des ondes*, Chapt. VI, Hermann et Cie, Paris, France, 1903.
34. Hashin, Z., "Analysis of Composite Materials—A Survey," *Journal of Applied Mechanics*, ASME, Vol. 50, 1983, pp. 481–505.
35. Hegemier, G. A., and Read, H. E., "Some Comments on Strain-Softening," *Report*, Univ. of California, San Diego, Calif., Oct., 1983, 19 pp.
36. Hill, A., "Acceleration Waves in Solids," *Journal of Mechanics and Physics of Solids*, Vol. 10, 1962, pp. 1–16.
37. Janson, J., and Hult, J., "Fracture Mechanics and Damage Mechanics—A Combined Approach," *Journal de Mécanique Appliquée*, Vol. 1, No. 1, 1977, pp. 69–84.
38. Kachanov, L. M., "Time of Rupture Process Under Creep Conditions," *Izvestia Akademii Nauk*, USSR, No. 8, 1958, pp. 26–31.
39. Krajcinovic, D., "Constitutive Equations for Damaging Materials," *Paper 83-APM-12*, presented at the June, 1983, ASME Applied Mechanics Conference, held in Houston, Tex; *Journal of Applied Mechanics*, ASME, in press.
40. Kröner, E., "Elasticity Theory of Materials with Long Range Cohesive Forces," *International Journal of Solids and Structures*, Vol. 3, 1967, pp. 731–742.
41. Kröner, E., "Interrelations Between Various Branches of Continuum Mechanics," *Mechanics of Generalized Continua*, E. Kröner, ed., Springer-Verlag, 1968, pp. 330–340.
42. Krumhansl, J. A., "Some Considerations of the Relation Between Solid State Physics and Generalized Continuum Mechanics," *Mechanics of Generalized Continua*, E. Kröner, ed., Springer-Verlag, 1968, pp. 298–311.
43. Kunin, I. A., "The Theory of Elastic Media with Microstructure and the Theory of Dislocations," *Mechanics of Generalized Continua*, E. Kröner, ed., Springer-Verlag, 1968, pp. 321–328.
44. Leckie, F. A., "Constitutive Equations of Continuum Creep Damage Mechanics," *Philosophical Transactions of Royal Society*, Ser. A, Vol. 288, London, 1978, pp. 27–47.
45. Leckie, F. A., and Onat, E. T., "Tensorial Nature of Damage Measuring Internal Variables," *Physical Nonlinearities in Structural Analysis*, J. Hult and J. Lemaitre, eds., Proceedings of the May, 1980, IUTAM Symposium held at Senlis, France, Springer Verlag, Berlin, 1981, pp. 140–155.
46. Lemaitre, J., "How to Use Damage Mechanics," (division lecture presented at SMiRT7, Chicago, 1983) *Intern. Report No. 40*, Laboratoire de Mécanique et Téchnologie, Ecole Normale Supérieure de l'Enseignement Technique, Paris, France, 1983.
47. Levin, V. M., "The Relation between Mathematical Expectation of Stress and Strain Tensors in Elastic Microheterogeneous Media," *Prikladnaya Mathematika i Mekhanika*, Vol. 35, 1971, pp. 694–701 (translated from the Russian).
48. Maier, G., "On Structural Instability due to Strain-Softening," IUTAM Symposium on Instability of Continuous Systems, held at Herrenhalb, Germany, Sept., 1969, Springer Verlag, West Berlin, 1971, pp. 411–417.
49. Maier, G., Zavelani, A., and Dotreppe, J. C., "Equilibrium Branching due to Flexural Softening," *Journal of the Engineering Mechanics Division*, ASCE, Vol. 99, No. EM4, Aug., 1978, pp. 897–901.
50. Mandel, J., "Conditions de stabilité et postulat de Drucker," *Rheology and Soil Mechanics*, J. Kravtchenko and P. M. Sirieys, eds., Proceedings of the 1964 IUTAM Symposium, held at Grenoble, France, Springer Verlag, Berlin, 1966, pp. 58–68.
51. Marchertas, A. H., Kulak, R. F., and Pan, Y. C., "Performance of Blunt Crack Approach within a General Purpose Code," *Nonlinear Numerical Analysis of Reinforced Concrete*, L. E. Schwer, ed., ASME, New York, N.Y., 1982, pp. 107–123.
52. Mazars, J., "Mechanical Damage and Fracture of Concrete Structures," 5th International Conference on Fracture, held at Cannes, France, 1981, D. François, ed., Vol. 4, pp. 1499–1506.
53. Mróz, Z., "Current Problems and New Directions in Mechanics of Geomaterials," *Mechanics of Geomaterials: Rocks, Concretes, Soils*, Z. P. Bažant, ed., J. Wiley, London, England (in press) (Proceedings of the Sept., 1983, IUTAM W. Prager Symposium, held at Northwestern University, Evanston, Ill.).
54. Palmer, A. C., and Rice, J. R., "The Growth of Slip Surfaces in the Progressive Failure of Overconsolidated Clay," Proceedings of the Royal Society, London, England, Series A, Vol. 332, 1973, pp. 527–548.
55. Pan, Y. C., Marchertas, A. H., and Kennedy, J. M., "Finite Element Analysis of Blunt Crack Band Propagation," *Preprints*, 7th International Conference on Structural Mechanics in Reactor Technology, Paper H, Chicago, Ill., Aug., 1983.
56. Pietruszczak, S., and Mróz, Z., "Finite Element Analysis of Deformation of Strain-Softening Materials," *International Journal for Numerical Methods in Engineering*, Vol. 17, 1981, pp. 327–334.
57. Rice, J. R., "The Localization of Plastic Deformation," *Theoretical and Applied Mechanics*, Preprints, IUTAM Congress held in Delft, 1976, W. T. Koiter, ed., North Holland, 1976, pp. 207–220.
58. Rudnicki, J. W., and Rice, J. R., "Conditions for the Localization of Deformation in Pressure Sensitive Dilatant Materials," *Journal of Mechanics and Physics of Solids*, Vol. 23, 1975, pp. 371–394.
59. Sandler, I., and Wright, J., "Summary of Strain-Softening," *Theoretical Foundations for Large-Scale Computations of Nonlinear Material Behavior, Preprints*, DARPA-NSF Workshop, S. Nemat-Nasser, ed., Northwestern University, Evanston, Ill., Oct., 1983, pp. 225–241.
60. Suaris, W., and Shah, S. P., "A Rate-Sensitive Damage Theory for Brittle Solids," *Journal of Engineering Mechanics*, ASCE, Vol. 110, No. 6, 1984, pp. 985–997.
61. Thomas, T. Y., *Plastic Flow and Fracture in Solids*, Academic Press, New York, N.Y., 1961.
62. Truesdell, C., and Noll, W., "The Nonlinear Theories of Mechanics," *Encyclopedia of Physics, Vol. III/3*, S. Flügge, ed., Springer Verlag, West Berlin, 1965.
63. Waversik, W. R., and Brace, W. F., "Post-Failure Behavior of Granite and Diabase," *Rock Mechanics*, Vol. 3, 1971, p. 61.
64. Wu, F. H., and Freund, L. B., "Deformation Trapping Due to Thermoplastic Instability in One-Dimensional Wave Propagation," *Journal of the Mechanics and Physics of Solids*, Vol. 32, No. 2, 1984, pp. 119–132.